Supplemental Material

Methods

Statistical Analysis. For testing of multiple linked parameters, the Wilcoxon signed rank test was performed after obtaining significance by Friedman ANOVA. *P* values were adjusted for multiple testing. The Mann-Whitney test was used to test for differences between two groups. The statistical tests used for each experiment are indicated in the figure legends. $P < 0.05$ was considered significant.

Cell lines. EBV-transformed B cell lines from donors with CGD and from HIV-infected and -uninfected individuals, T cell lymphoblastoid leukemia cell lines CEM-NKr-CCR5 (HIV-uninfected) and CEM-IIIB (HIV-infected), T cell lines (A3.01, Jurkat, and MT-2), B cell lines (Raji and Ramos), non-lymphocytic human cells and cell lines (human aortic endothelial cells, HAEC, human umbilical vein endothelial cells, HUVEC, human proximal tubular epithelial cells, PTEC, human lung adenocarcinoma epithelial cells, A549, human colorectal adenocarcinoma epithelial cells, CaCo2, and human foreskin fibroblasts) were used in the study.

Humanized NOD scid gamma (NSG) mice. Animal protocols were approved by the Institutional Animal Care and Use Committee, University of Maryland School of Medicine. Immunodeficient mice from the strain NOD.Cg-Prkdc^{scid} Il2rg^{tm1Wjl}/SzJ (NSG) were humanized by intraperitoneal injection of $10x10^6$ PBMCs from an HIV-negative donor. Three weeks later, the mice were screened for engraftment of human cells and then injected with 180µg of fluorescently labeled (Alexa Fluor 647, AF647) PGT151 or IgG antibody (control) via retroorbital injection. One hour

after the injection, blood samples from 10 mice (5 per each antibody) were collected and analyzed by FACS.

Preparation and cultivation of cells. Peripheral blood mononuclear cells (PBMCs) were obtained by leukapheresis and ficoll-hypaque centrifugation. $CD4^+$ T cells and NK cells were isolated using a cell separation system (StemCell Technologies). Cell lines, PBMCs and $CD4^+$ T cells were cultured in RPMI 1640-based medium. Stimulation of cells was performed using the following reagents: T-cell specific stimulation was accomplished with the use of 5μg/ml of anti-CD3 antibody (BD Pharmingen) and 1μg/ml of anti-CD28 antibody (BD Pharmingen) in the presence of 20U/ml of interleukin 2 (IL-2), B-cell specific stimulation required 10μg/ml of goat $F(ab')_2$ anti-human IgG/A/M (Jackson ImmunoResearch Laboratories). α-mannosidase I inhibitor kifunensine (EMD Millipore) was used at a concentration of 2μg/ml.

Flow Cytometric Analysis. bNAbs (PGT121, 10-1074, VRC01, 3BNC117, PG9, PG16, 10E8) were obtained from the AIDS Reagent Program. bNAbs (PGT151, VRC26.09, 35O22) were obtained from the Vaccine Research Center, NIAID, NIH. Human IgG (ChromPure Human IgG, Jackson ImmunoResearch Laboratories) was used as a negative control. Of note, the differences in the level of binding of human polyclonal IgG versus monoclonal IgG1 to $CD4^+$ and $CD8^+$ T cells of HIV-uninfected donors were negligible. 10μg/ml of bNAbs or human IgG (control) was used for FACS analysis. Detection of these antibodies was mediated by allophycocyanin (APC) $F(ab')_2$ fragment goat anti-human IgG, Fcγ fragment specific secondary antibody (Jackson ImmunoResearch Laboratories), or by direct conjugation of bNAb with Alexa Fluor 488 fluorophore using APEX Antibody Labeling Kit (Invitrogen). PBMCs were stained with the

following fluorophore-conjugated antibodies: CD3-BV510 (clone OKT3, Biolegend), CD4-PE (clone RPA-T4, BD Pharmingen), CD8-BV421 (clone RPA-T8, BD Horizon), CD19-PerCP-Cy5.5 (clone SJ25C1, eBioscience). For T cell subset analysis, the following fluorophore-conjugated antibodies were used: CD3-BV510 (clone OKT3, Biolegend), CD4-PerCP (clone SK3, BD Biosciences), CD19-BV421 (clone HIB19, BD Pharmingen), CD45RA-PeCy7 (clone HI100, BD Pharmingen), CD27-APC (clone M-T271, BD Pharmingen), CCR7-PE (clone 3D12, eBioscience). The subsets were defined as follows: Naïve (CD45RA+, CCR7+, CD27+), T_{EMRA} (CD45RA+, CCR7-), T_{CM} (CD45RA-, CCR7+, CD27+), T_{TM} (CD45RA-, CCR7-, CD27+), and T_{EM} (CD45RA-, CCR7-, CD27-). For activation markers staining, the following fluorophore-conjugated antibodies were used: CD69-PE (clone L78, BD Biosciences), CD25-PE-Cy7 (clone M-A251, BD Biosciences). Highly enriched NK cells were pretreated with Fc Receptor Blocking Solution (Human TruStain FcX, Biolegend) or Anti-Human Fc Receptor Binding Inhibitor (eBioscience) according to manufacturer's instructions, and stained with different directly conjugated bNAbs and CD16-PeCy7 (clone 3G8, Biolegend). Data were acquired on a BD FACSCanto II flow cytometer using the FACSDiva software (Becton Dickinson) and analyzed using Flow Jo version 10.1r5 (Treestar, LLC USA) .

NK cell degranulation and cell death. Highly enriched NK cells (3.5×10^5 cells per well) were incubated with bNAbs or control IgG (1.5µg/ml) in U-bottom 96-well plate at 37°C. After 2h, cells were stained with CD107a-PerCP antibody (clone H4A3, Biolegend) to assess NK degranulation and with CD16-PeCy7 (clone 3G8, Biolegend), CD56-FITC (clone HCD56, Biolegend), CD57-BV421 (clone NK1, BD Horizon), NKG2A-APC (R&D systems), NKG2D-PE (clone 1D11, Biolegend), and NKG2C-PE (R&D systems) antibodies to evaluate NK cell

phenotype. After 6h, cells were stained with SYTOX Orange dead cell stain (Invitrogen) to assess NK cell death. Data were acquired on a BD FACSCanto II flow cytometer using the FACSDiva software (Becton Dickinson) and analyzed using Flow Jo version 10.1r5 (Treestar, LLC USA).

Supplemental Figures

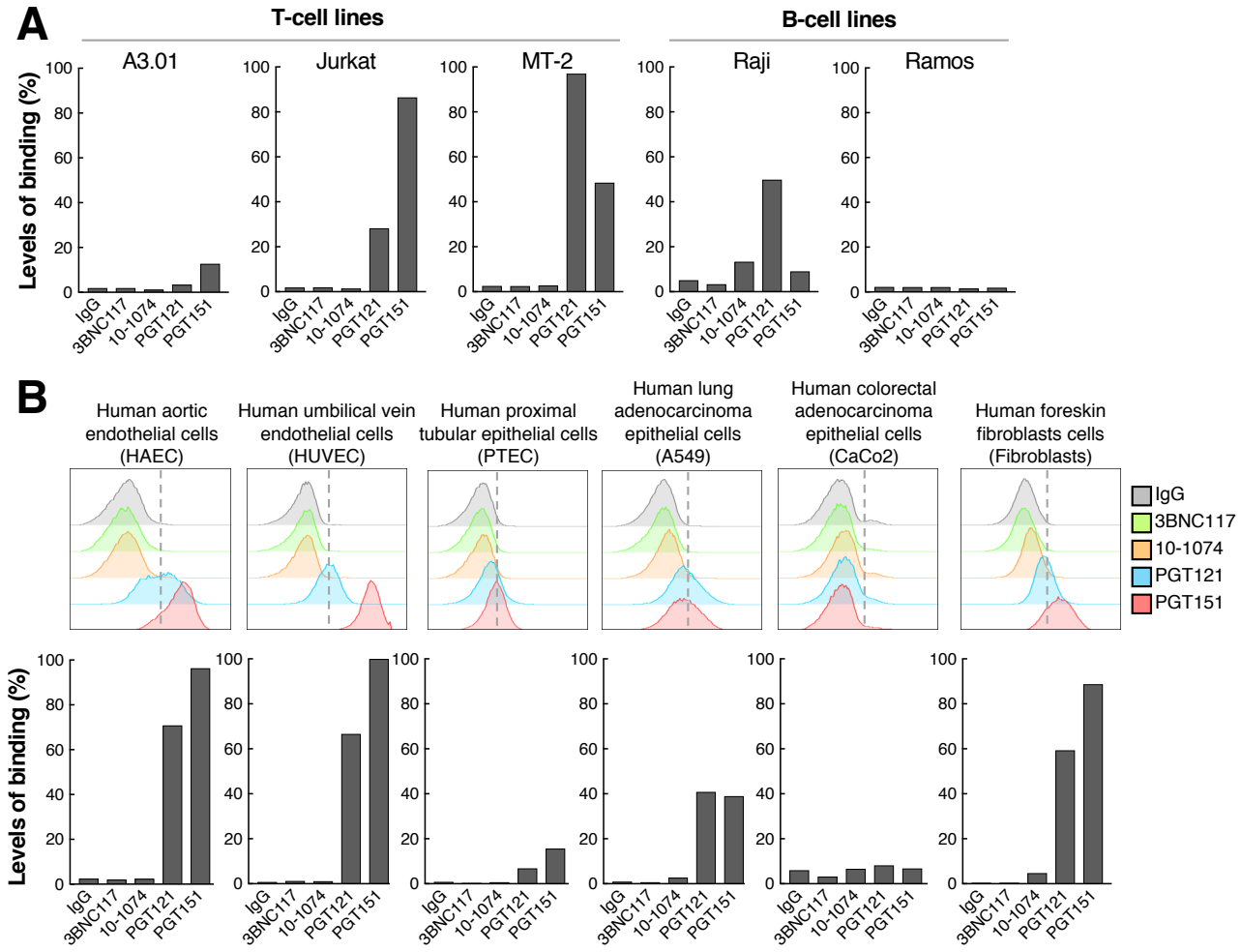

Supplemental Figure 1. Binding of bNAbs to T and B cell lines and to non-lymphocytic human cells and cell lines. Levels of binding of IgG (negative control) and bNAbs (3BNC117, 10-1074, PGT121, and PGT151) to (**A**) T cell lines A3.01, Jurkat, and MT-2 and B cell lines Raji and Ramos, and to (**B**) human aortic endothelial cells, HAEC, human umbilical vein endothelial cells, HUVEC, human proximal tubular epithelial cells, PTEC, human lung adenocarcinoma epithelial cells, A549; human colorectal adenocarcinoma epithelial cells, CaCo2, and human foreskin fibroblasts are shown.

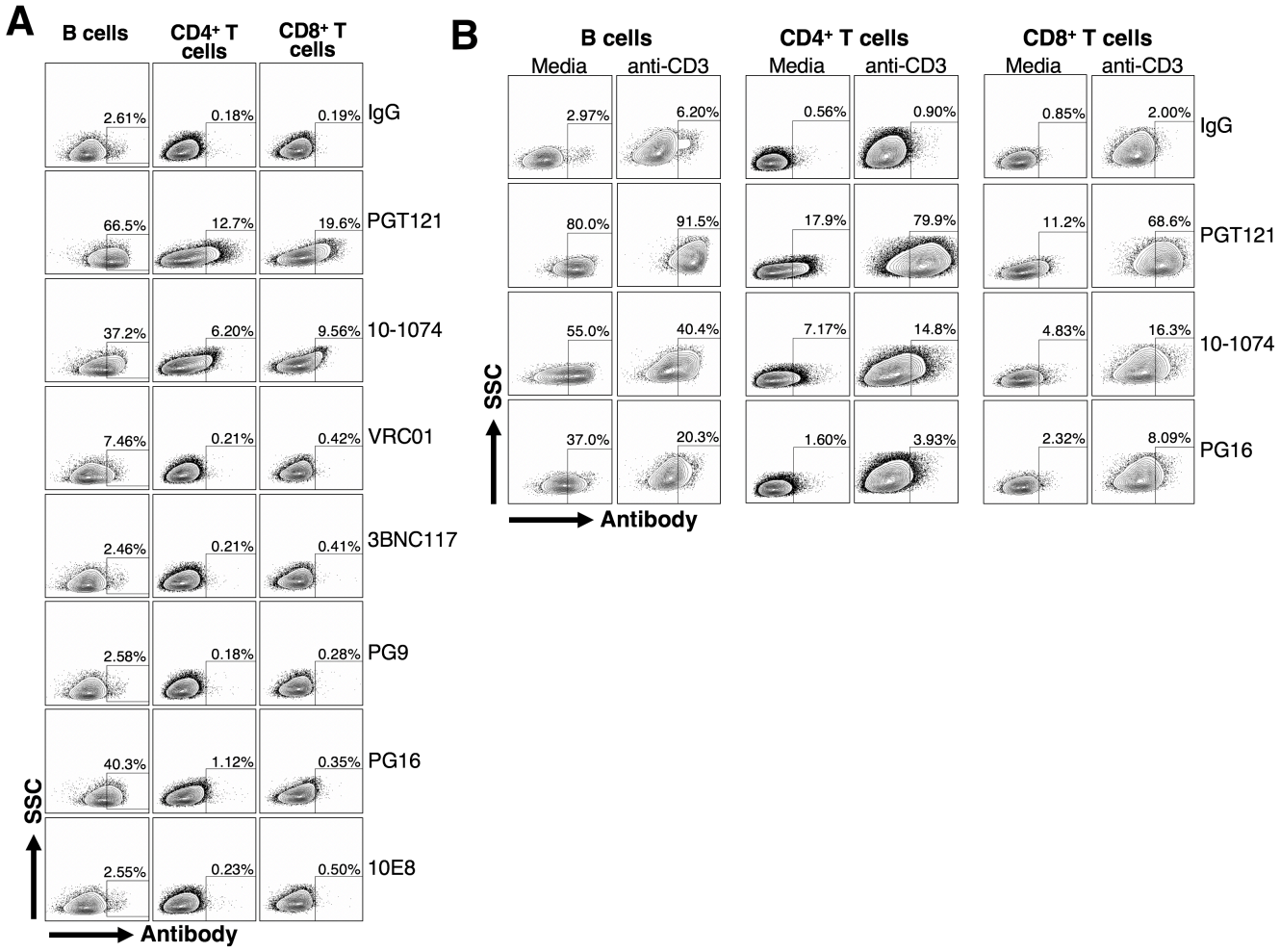

Supplemental Figure 2. Representative FACS plots of binding of bNAbs to lymphocytes of HIV-uninfected individuals. (**A**) Binding of IgG (negative control) and bNAbs (PGT121, 10-1074, VRC01, 3BNC117, PG9, PG16 and 10E8) to B cells, $CD4^+$ T cells, and $CD8^+$ T cells in freshly isolated PBMCs of HIV-uninfected donors. (**B**) Binding of IgG, PGT121, 10-1074 and PG16 to unstimulated (Media) and anti-CD3 stimulated B cells, $CD4^+$ T cells and $CD8^+$ T cells.

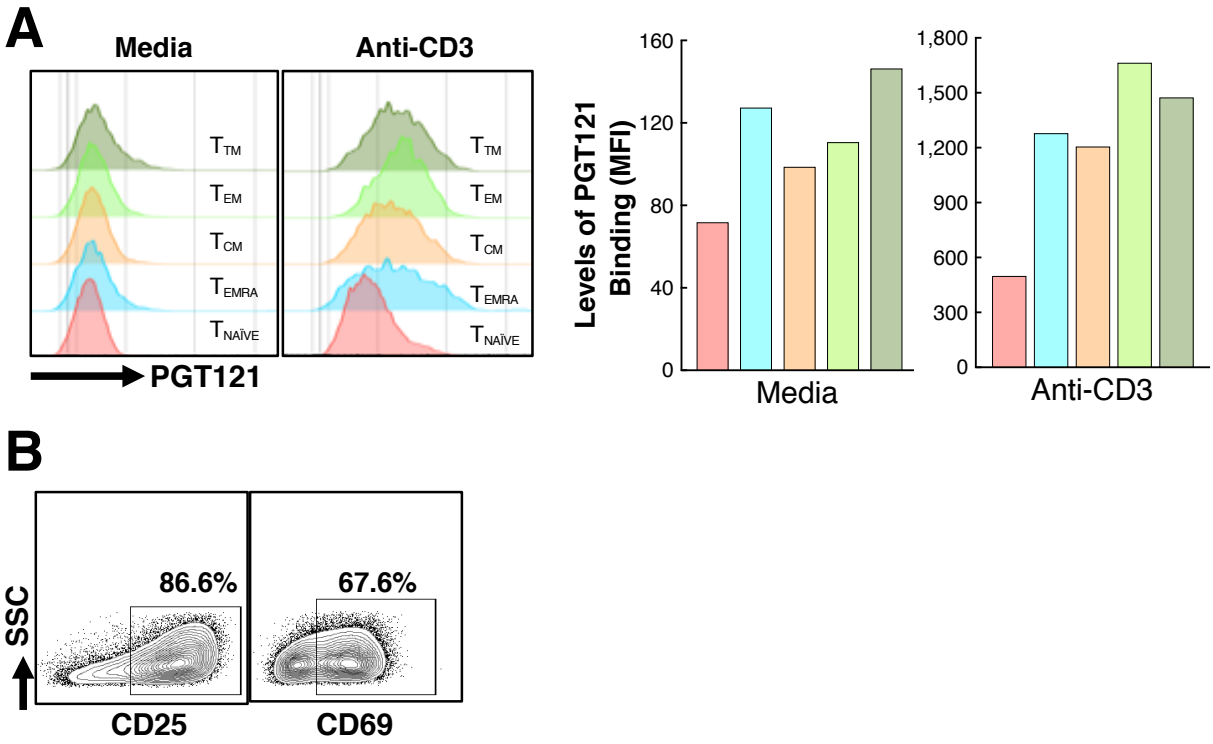

Supplemental Figure 3. PGT121 binding to subsets of CD4$^+$ T cells. (**A**) Levels of PGT121 binding to different CD4$^+$ T cell subsets: Naïve (red), Effector memory RA$^+$ (T_{EMRA}; blue), Central memory (T_{CM}; orange), Transitional memory (T_{TM}; light green), Effector memory (T_{EM}; dark green), without stimulation (Media) and 2 days after stimulation with anti-CD3 antibody. The data are shown in histograms and mean fluorescent intensity (MFI). (**B**) Expression of activation markers CD25 and CD69 on PGT121$^+$ CD4$^+$ T cells.

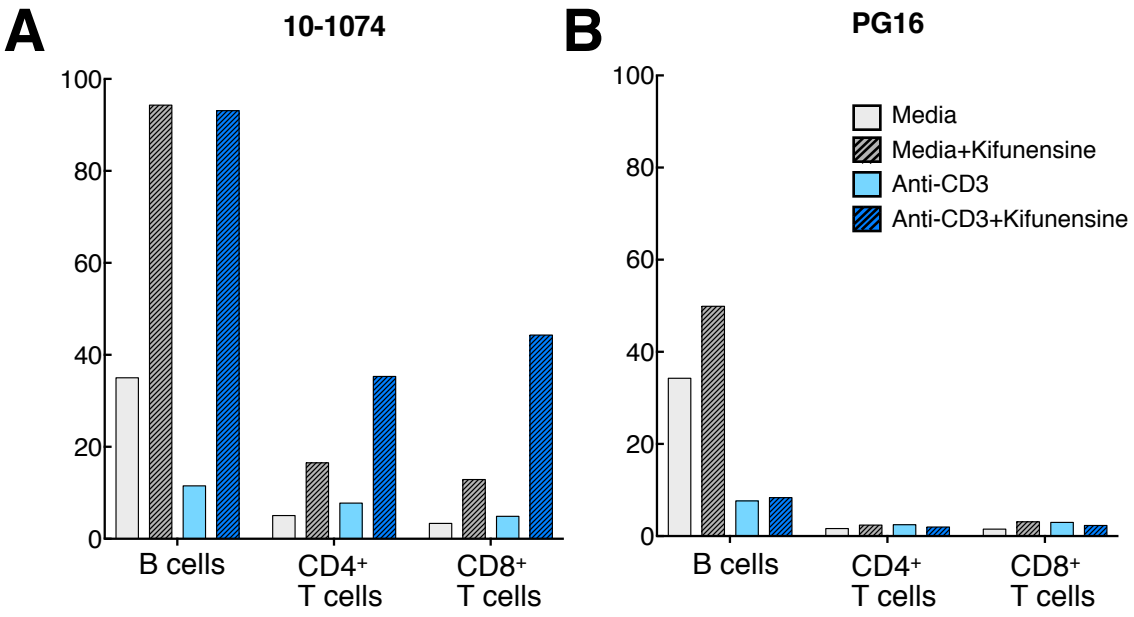

Supplemental Figure 4. Effect of glycosylation on binding of 10-1074 and PG16. Levels of binding of 10-1074 (**A**), and PG161 (**B**) to the unstimulated (Media; in grey) and stimulated (anti-CD3 antibody; in blue) B cells, $CD4^+$ and $CD8^+$ T cells in the presence (hatched bars) or absence (solid bars) of kifunensine.

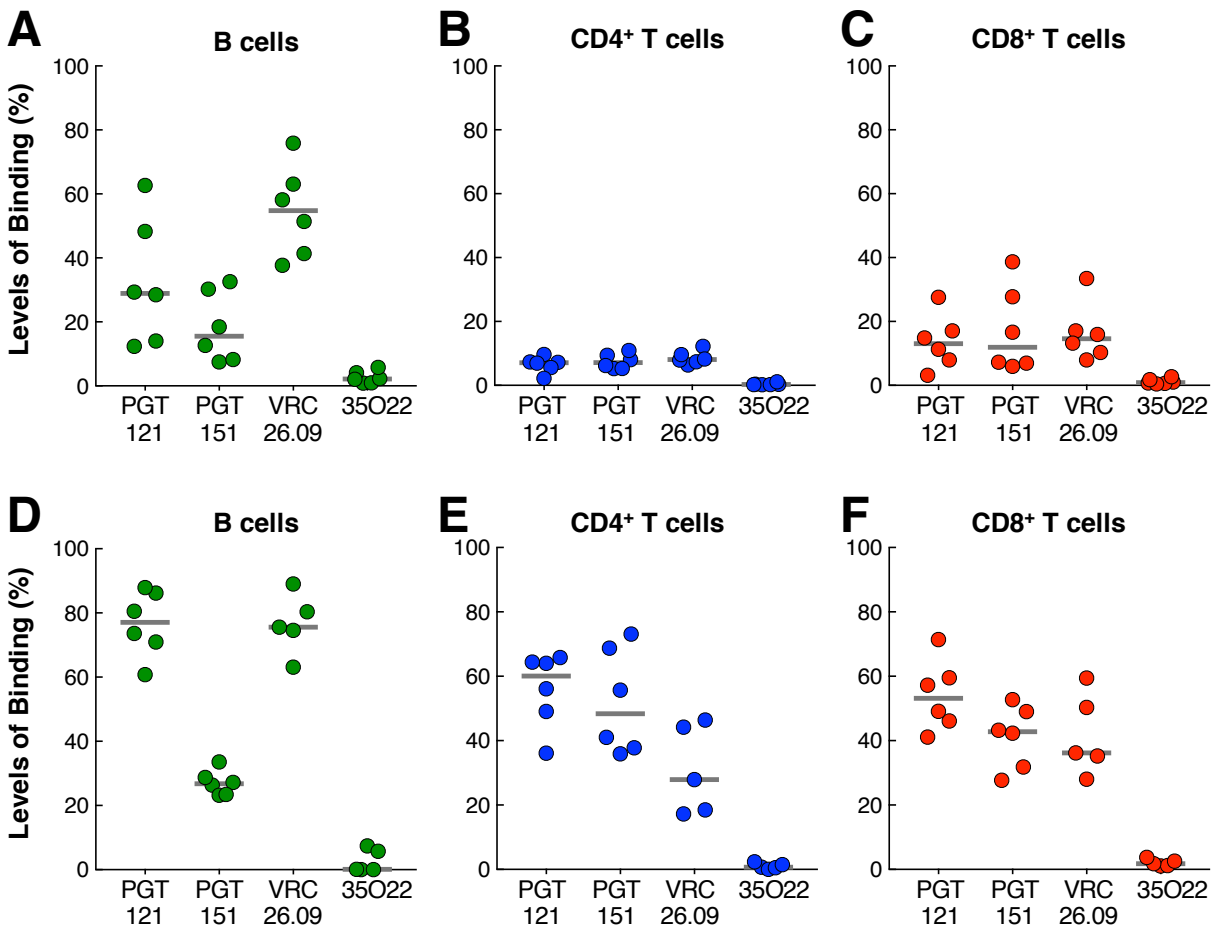

Supplemental Figure 5. Complex-type glycan specific bNAbs binding to lymphocytes of HIV-uninfected individuals. (**A**-**C**) Levels of PGT121, PGT151, VRC26.09, and 35O22 to B cells (**A**), CD4$^+$ T cells (**B**) and CD8$^+$ T cells (**C**) in PBMCs from HIV-negative donors. (**D**-**F**) Binding of PGT121, PGT151, VRC26.09, and 35O22 to B cells (**D**), CD4$^+$ T cells (**E**), and CD8$^+$ T cells (**F**) in PBMCs from HIV-negative donors 2 days after stimulation with anti-CD3 antibody.

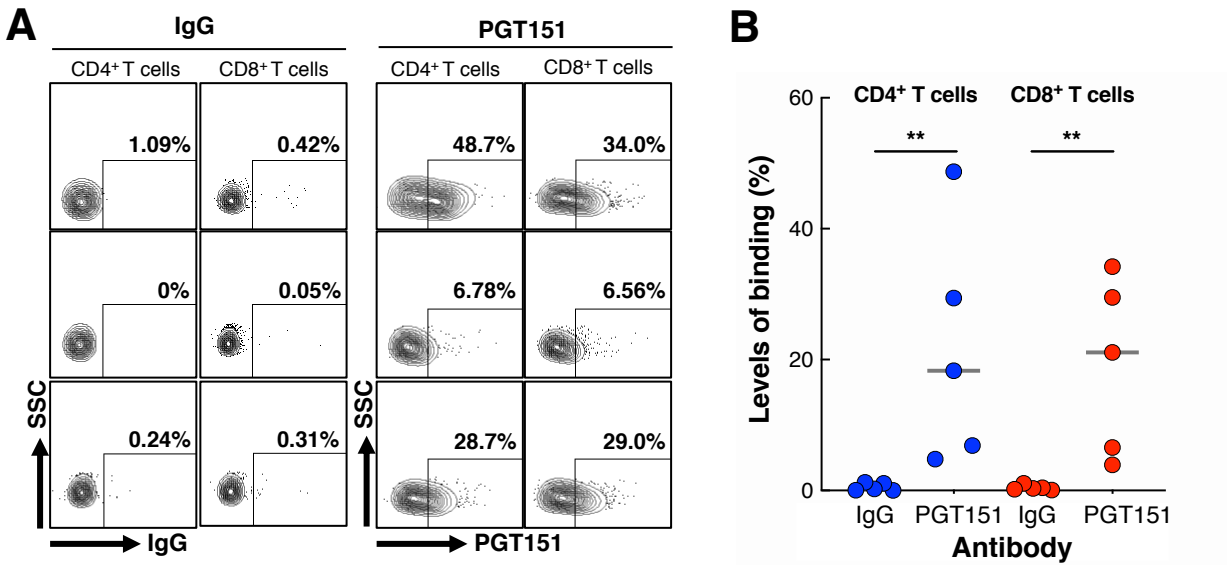

Supplemental Figure 6. PGT151 binding to T cells in humanized NSG mice. Three weeks following injection of PBMCs of HIV-uninfected individuals into mice, fluorescently conjugated PGT151 was administered to the mice and blood samples were subjected to flow cytometric analysis. Fluorescently conjugated human IgG was used as a negative control. **(A)** Representative FACS plots of human IgG and PGT151 binding to $CD4^+$ and $CD8^+$ T cells in humanized NSG mice. **(B)** Levels of IgG and PGT151 binding to $CD4^+$ (blue) and $CD8^+$ (red) T cells in 10 mice (5 per group). Statistical significance was tested with the Mann-Whitney test . $^{**}P = 0.0079$.

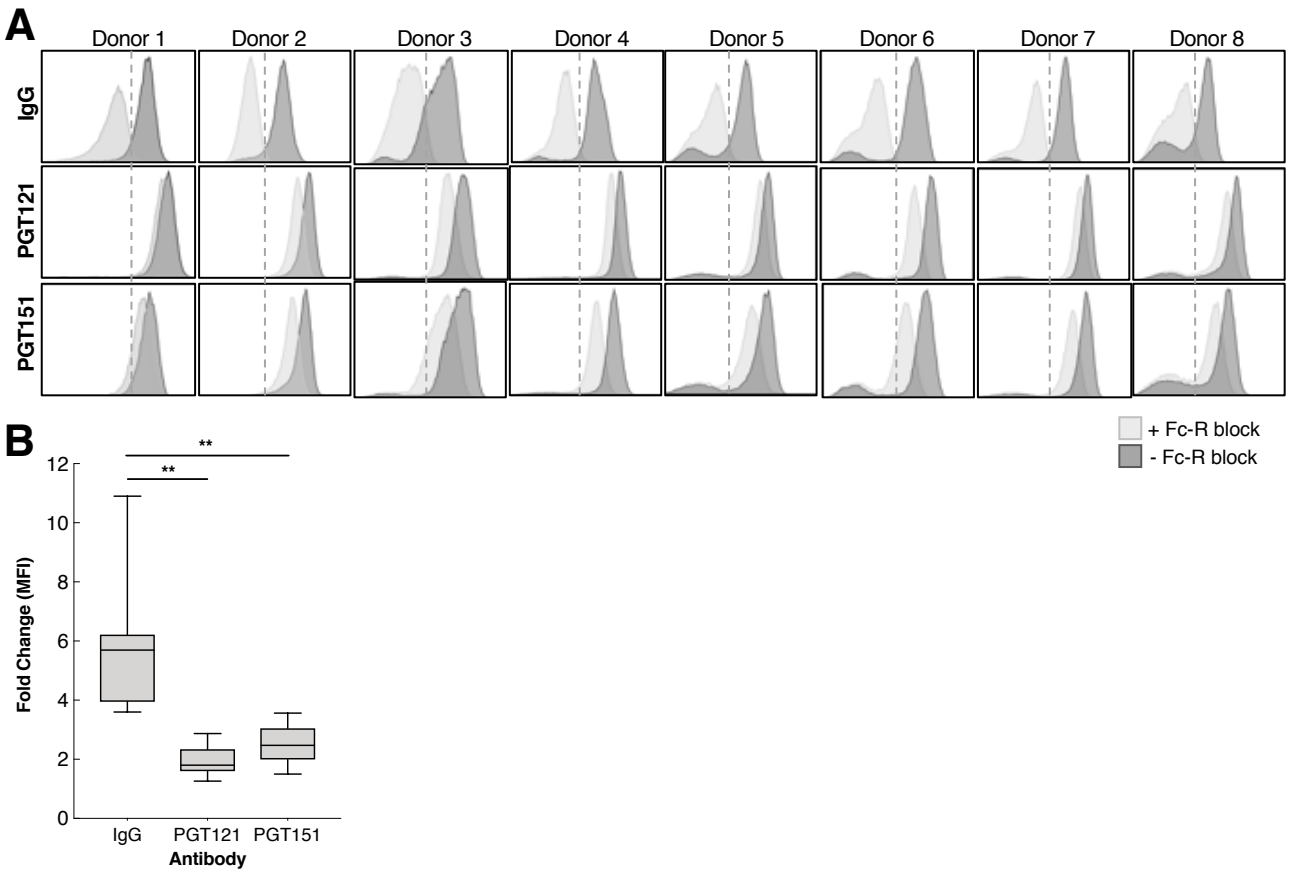

Supplemental Figure 7. Comparison of binding of human IgG and bNAbs (PGT121 and PGT151) to NK cells in the presence and absence of Fc-receptor blocker. (**A**) Representative FACS plots (histogram) of binding of human IgG (negative control) and PGT121 and PGT151 to NK cells in the presence (light grey) and absence (dark grey) of Fc-receptor blocker. (**B**) Fold changes in mean fluorescence intensity (MFI) of binding of IgG, PGT121, and PGT151 in the presence and absence of Fc-receptor blocker. Statistical significance was tested with Wilcoxon matched-pairs signed rank test. $^{**}P = 0.0078$.

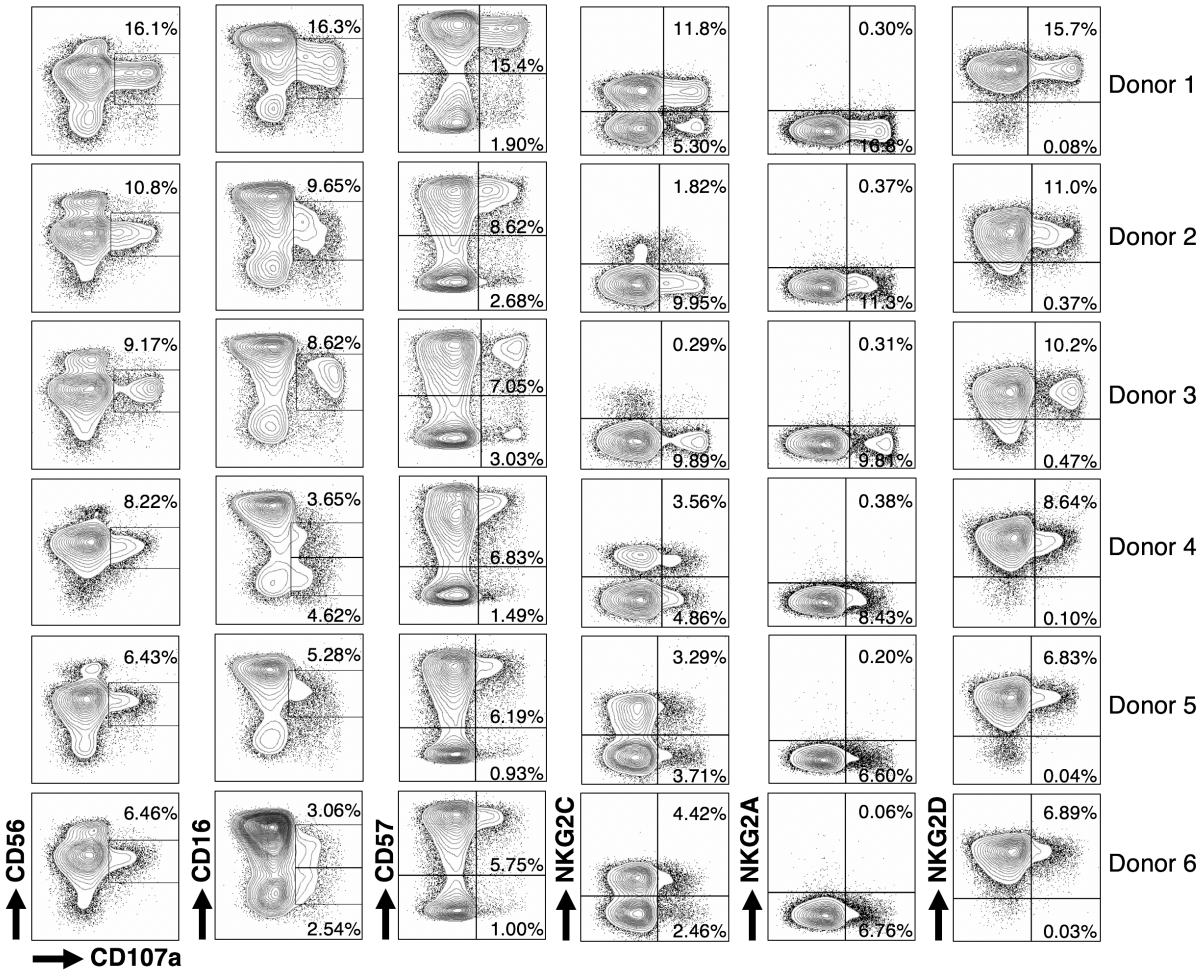

Supplemental Figure 8. Phenotypic characterization of NK cells undergoing degranulation upon incubation with PGT151. The level of degranulation (CD107a^{+}) is shown on the X axis and markers of NK cells (CD56, CD16, CD57, NKG2C, NKG2A and NKG2D) are shown on the Y axes.

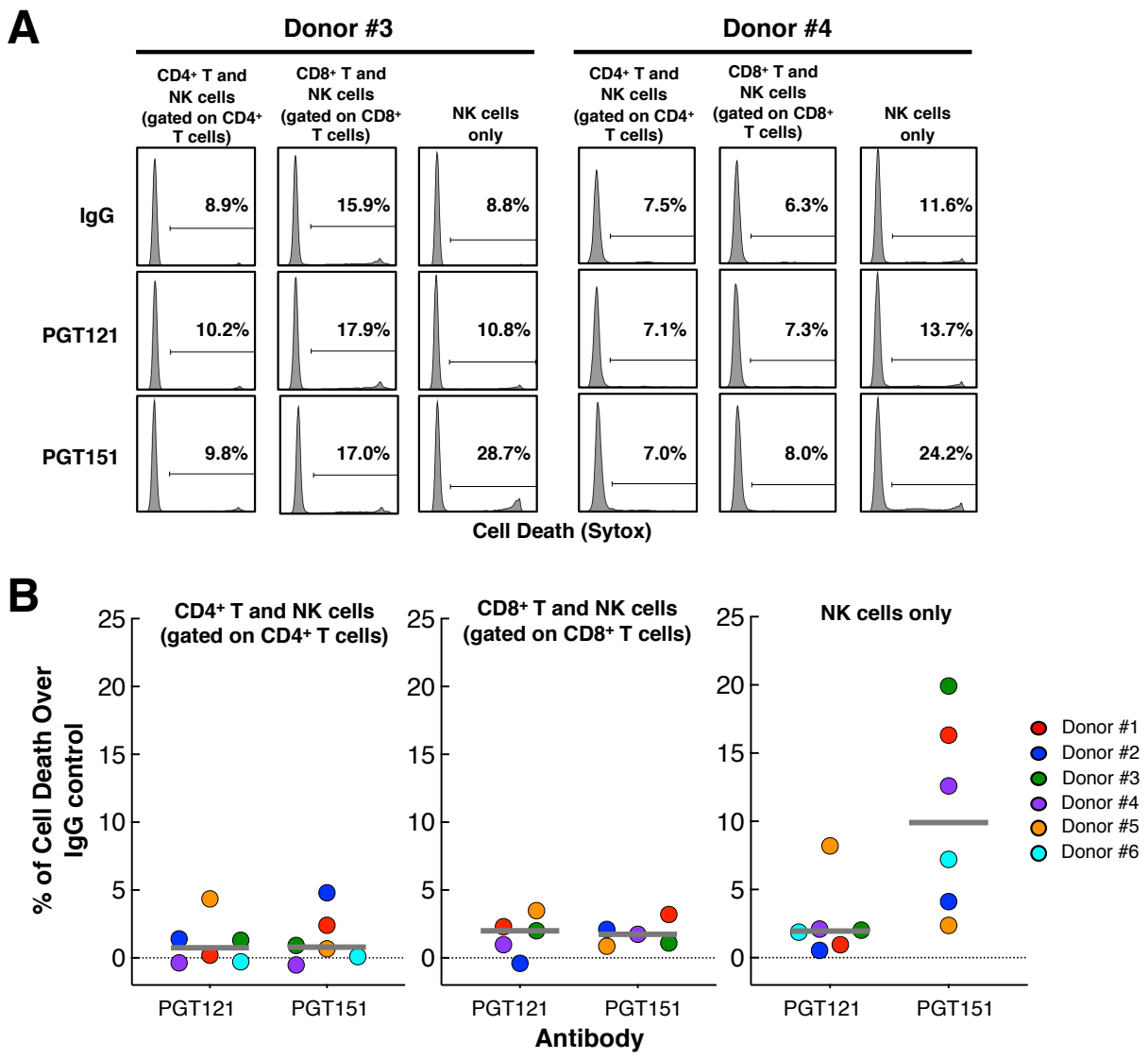

Supplemental Figure 9. Levels of NK cell-mediated killing against lymphocyte targets. Anti-CD3 antibody stimulated $CD4^+$ and $CD8^+$ T cells and NK cells obtained from 6 HIV-uninfected donors were incubated with either PGT121 or PGT151. After 6h incubation, the level of cell death was measured by staining cells with a nucleic acid dye Sytox.